Mathematical Biosciences and Engineering

http://www.aimspress.com/journal/mbe

MBE, 20(10): 17783–17802.
DOI: 10.3934/mbe.2023790
Received: 15 June 2023
Revised: 14 August 2023
Accepted: 11 September 2023
Published: 18 September 2023

Research article

Media impact research: a discrete SIR epidemic model with threshold switching and nonlinear infection forces

Wenjie Qin[1], **Jiamin Zhang**[2] **and Zhengjun Dong**[1,*]

[1] Department of Mathematics, Yunnan Minzu University, Kunming 650500, China
[2] College of Science, China Three Gorges University, Yichang 443000, China

* **Correspondence:** Email: zjdong0209@163.com.

Abstract: The media's coverage has the potential to impact human behavior and aid in the control of emergent infectious diseases. We aim to quantify and evaluate the extent to which media coverage can influence infectious disease control through a mathematical model, thus proposing a switching epidemic model that considers the effect of media coverage. The threshold strategy incorporates media influence only when the number of infected cases surpasses a specific threshold; otherwise, it is disregarded. When conducting qualitative analysis of two subsystems, focusing on the existence and stability of equilibria. Using numerical methods, the codimension-2 bifurcation analysis is adopted here to investigate the various types of equilibria within the switching system that play a vital role in pest control. On the other hand, codimension-1 bifurcation analysis reveals the existence of periodic, chaotic solutions, period-doubling bifurcations, multiple attractors and other complexities within the proposed model, which could pose challenges in disease control. Additionally, the impact of key parameters on epidemic outbreaks is analyzed, such as the initial values of susceptible and infective individuals, and discuss the potential benefits of mass media coverage in preventing emerging infectious diseases. The modeling and analytical techniques developed for threshold control strategies can be applied to other disease control efforts.

Keywords: media reports; switched epidemic model; threshold strategy; bifurcation analysis

1. Introduction

Infectious diseases have been a long-standing threat to human beings, claiming countless lives and causing catastrophic consequences for human survival and development. For instance, the Antonine plague in ancient Rome in 164 AD [1] resulted in numerous deaths, weakened the strength of ancient Rome to a certain extent and indirectly contributed to the decline of the Roman Empire. Similarly, the Black Death outbreaks in Europe between 1347–1353 [2] killed about one-third of the European population. The outbreak of SARS in 2003 [3] caused significant fatalities and economic losses. The

H1N1 influenza virus that emerged in Mexico in 2009 [4] can cause pneumonia, leading to respiratory failure and multiple organ damage, resulting in death for some infected individuals. Moreover, the sudden onset of COVID-19 in 2020 [5–8] has had a profound impact on human health, the global economy and social behavior. These diseases have undoubtedly inflicted an incalculable toll on economic development and people's lives. Therefore, it is essential to investigate the spread of infectious diseases and propose effective prevention and control strategies. The study of infectious diseases has become crucial to address the long-standing problem of fulminant diseases that have plagued humanity. Since experimental research on infectious diseases is often challenging, appropriate mathematical models are frequently employed to reflect the transmission mechanism of diseases. The dynamic model of infectious disease is an effective approach commonly utilized in the theory and qualitative analysis of infectious disease [9]. By conducting qualitative and quantitative analyses of the model dynamics and numerical simulations, the critical factors affecting the spread of infectious diseases can be identified and the future development trend can be predicted. This provides strong theoretical and data support for the prevention and control of infectious diseases, enabling accurate and effective disease prevention.

The spread of infectious diseases is influenced by numerous factors, including media reports [10–15], population density [16] and vaccination [17]. In modern times, the media plays a significant role in shaping people's lifestyles, and its impact on the spread of infectious diseases is crucial. During an epidemic of infectious diseases, people often rely on the media, including news and broadcasts, to share information about disease prevention, control and their own experiences in fighting the disease. The media reports the spread of diseases promptly and through various channels, and people take appropriate measures, such as wearing masks, maintaining personal hygiene, reducing visits to public places and frequently washing their hands, to prevent and reduce the spread and occurrence of diseases [18]. Thus, it is practical to consider the influence of media factors in the infectious disease model and to optimize the control strategy of infectious diseases to obtain reasonable prevention and control measures.

There are various types of infectious disease models that can be influenced by media reports, such as continuous models, switched models and discrete models. However, researchers typically opt to use continuous models to study the influence of media coverage on disease transmission. In 2007, Liu et al. [19] conducted pioneering research on the influence of media and psychological effects on infectious diseases. They proposed a continuous infectious disease model with an infectious rate of $\beta e^{a_1 E - a_2 I - a_3 H}$. In 2008, Cui et al. [20] introduced a media influence function of βe^{-mI} and developed a continuous SEI model. The variable m represents the psychological reaction of the public after learning about the disease through media reports. The dynamic behavior of the model was analyzed with varying values of m to evaluate the influence of media on the spread and control of the disease. Furthermore, switching models have also been studied by many researchers, in combination with other factors. A switching system is generally composed of some subsystems and a switching signal [21, 22]. Its main feature is that the rich dynamic behavior of the original system becomes more complicated under the action of the switching signal. In 2013, Xiao et al. [23] established a continuous infectious disease model with a media impact factor $M(I, dI/dt)$, and studied the role of the media and behavioral changes of consciousness by considering the existence of a threshold for susceptibles. They then transformed the model into a switching system and concluded that media or psychological influence will delay the peak of the epidemic and cause a small-scale disease outbreak. Liu et al. [24] established a SIR epidemic model having a non-smooth function $f(I)$ and analyzed the dynamics of the infectious disease switching system through a saturation function to explore the impact of media reports on the spread of infectious

diseases. Zhao [25] considered the media impact factor function $\beta(I) = \beta/(1 + \varepsilon mI)$ to establish a Filippov model with a media switching threshold strategy. They concluded that the greater the media's propaganda, the more beneficial the disease control and elimination.

The aforementioned work is based on research and analysis conducted using either a continuous model or a continuous switching model. When the population size is large, the changes in the number of susceptible and infected individuals can be approximated as continuous over time, making it reasonable to use a continuous model. However, when the spread of infectious diseases is slow, or data collection occurs on a yearly, monthly, weekly or daily basis, population changes occur discretely rather than continuously. Therefore, using discrete models to describe the dynamic behavior of infectious diseases is more appropriate in such situations. These models can also provide more effective and accurate data references for subsequent disease prevention and control measures.

Compared to continuous infectious disease models, there are fewer studies on discrete infectious disease models [26, 27]. Moreover, there are even fewer studies on discrete switching infectious disease models that take into account the influence of media reports. In this study, we will focus on the discrete infectious disease switching model that incorporates a media influence factor of βe^{-mI}. To better reflect real-world scenarios, we consider a switching model that includes the economic threshold (ET) [28, 29] of infected individuals. We explore the dynamic behavior of the system when the number of infected individuals exceeds the critical ET. The objective is to investigate the impact of media reports on the epidemic trend of infectious diseases, analyze the dynamic behaviors arising from influential factors and provide effective strategies for prevention and control of infectious disease to keep the number of infected individuals within a desired threshold level.

The rest of the paper is structured as follows. In the next section, we propose a non-smooth infectious disease switching model that can effectively capture the influence of media reports. In Section 3, we provide a qualitative analysis of the two subsystems. Section 4 is devoted to numerical simulations to explore the impact of initial population density on disease outbreaks and to analyze the bifurcation of sensitive parameters. Finally, we conclude the paper with a discussion of our findings and their implications for infectious disease prevention and control measures in the last section.

2. Establishment of discrete switched epidemic model

Kermack and McKendrick introduced the SIR compartment model [30] in 1927, which has become a popular tool for studying infectious diseases. One of its key assumptions is that individuals who recover from the disease will develop lifelong immunity, as seen in diseases such as chickenpox and measles. Building on this, the SIR continuous model can be formulated by the following equation set:

$$\begin{cases} S'(t) = \Lambda - \beta S(t)I(t) - \mu S(t), \\ I'(t) = \beta S(t)I(t) - (\mu + \delta + \gamma)I(t), \\ R'(t) = \gamma S(t) - \mu R(t), \end{cases} \tag{2.1}$$

where $S(t), I(t)$ and $R(t)$ respectively represent the number of susceptibles, infected individuals and recoveries at time t; Λ is the recruitment rate of the individuals at a time, β is infection rate, μ is the natural death rate, δ is the mortality rate due to disease and γ is the recovery rate from infection.

Due to the discontinuity of data collection units and changes in population, we adopt a discrete-time infectious disease model to better reflect the actual situation. There are several approaches to building

a discrete model, but the most commonly used method is to discretize a continuous model. The two commonly used methods are the Mickens non-standard discrete method and the Euler discrete method. Motivated by [31–33], the Euler method was used to discretize the model (2.1). The resulting discrete model is shown below:

$$\begin{cases} S_{n+1} = S_n + \Lambda - \beta S_n I_n - \mu S_n, \\ I_{n+1} = I_n + \beta S_n I_n - (\mu + \delta + \gamma) I_n, \\ R_{n+1} = R_n + \gamma I_n - \mu R_n. \end{cases} \tag{2.2}$$

Based on model (2.2), we now incorporate the effect of media influence factor m by modifying the infection rate β to βe^{-mI}. The updated model is expressed as follows

$$\begin{cases} S_{n+1} = S_n + \Lambda - \beta e^{-mI} S_n I_n - \mu S_n, \\ I_{n+1} = I_n + \beta e^{-mI} S_n I_n - (\mu + \delta + \gamma) I_n, \\ R_{n+1} = R_n + \gamma S_n I_n - \mu R_n. \end{cases} \tag{2.3}$$

Typically, there is no media coverage when the quantity of infected individuals is small and does not exceed the ET. In such cases, the disease fails to capture the attention of the public at large. However, once the number of infected individuals abruptly surges and surpasses the ET, the role of media influence becomes significant. Media reports and publicity can draw the public's attention towards the disease dynamics and prompt individuals to alter their behavior and take appropriate protective measures.

Taking advantage of the threshold policy, we combine models (2.2) and (2.3) as follows

$$\begin{cases} \left.\begin{aligned} S_{n+1} &= S_n + \Lambda - \beta S_n I_n - \mu S_n, \\ I_{n+1} &= I_n + \beta S_n I_n - (\mu + \delta + \gamma) I_n, \\ R_{n+1} &= R_n + \gamma I_n - \mu R_n, \end{aligned}\right\} I_n < ET, \\ \left.\begin{aligned} S_{n+1} &= S_n + \Lambda - \beta e^{-mI} S_n I_n - \mu S_n, \\ I_{n+1} &= I_n + \beta e^{-mI} S_n I_n - (\mu + \delta + \gamma) I_n, \\ R_{n+1} &= R_n + \gamma I_n - \mu R_n, \end{aligned}\right\} I_n \geq ET. \end{cases} \tag{2.4}$$

Note that the first two equations of models (2.2) and (2.3) do not involve the variable R. To simplify model (2.4), we can express it as

$$\begin{cases} \left.\begin{aligned} S_{n+1} &= S_n + \Lambda - \beta S_n I_n - \mu S_n, \\ I_{n+1} &= I_n + \beta S_n I_n - (\mu + \delta + \gamma) I_n, \end{aligned}\right\} I_n < ET, \\ \left.\begin{aligned} S_{n+1} &= S_n + \Lambda - \beta e^{-mI} S_n I_n - \mu S_n, \\ I_{n+1} &= I_n + \beta e^{-mI} S_n I_n - (\mu + \delta + \gamma) I_n, \end{aligned}\right\} I_n \geq ET. \end{cases} \tag{2.5}$$

The discrete switching model (2.5) expresses a dynamic system that adheres to a threshold policy, whereby media influence is only effective when $I_n \geq ET$. For more information on the threshold policy, please refer to [28, 29]. Similar modeling approaches can also be found in the literature, such as in references [34, 35].

3. Dynamic behavior analysis of subsystems

The two subsystems of discrete switching model (2.5) are qualitatively analyzed, including existence and stability, to explore the complex dynamic behavior of the model in this section.

Denoting $F(Z) = I_n - ET$ with vector $Z = (S_n, I_n)^T$, and

$$S_{G_1}(Z) = \begin{bmatrix} S_n + \Lambda - \beta S_n I_n - \mu S_n \\ I_n + \beta S_n I_n - (\mu + \delta + \gamma) I_n \end{bmatrix}, \tag{3.1}$$

$$S_{G_2}(Z) = \begin{bmatrix} S_n + \Lambda - \beta e^{-mI} S_n I_n - \mu S_n \\ I_n + \beta e^{-mI} S_n I_n - (\mu + \delta + \gamma) I_n \end{bmatrix}, \tag{3.2}$$

so switching system (2.5) can be rewritten as a vector

$$Z'(t) = \begin{cases} S_{G_1}(Z), & Z \in G_1, \\ S_{G_2}(Z), & Z \in G_2, \end{cases} \tag{3.3}$$

where

$$G_1 = \left\{ Z \in \mathbb{R}^2_+ : F(Z) < 0, S_n > 0, I_n > 0, \right\}. \tag{3.4}$$

$$G_2 = \left\{ Z \in \mathbb{R}^2_+ : F(Z) \geq 0, S_n > 0, I_n > 0. \right\}. \tag{3.5}$$

Using the threshold policy, we define regions G_1 and G_2 of system (3.3) as S_{G_1} and S_{G_2}, respectively. Subsequently, we will investigate the dynamical behavior of subsystems S_{G_1} and S_{G_2}. Below, we present the definition of regular equilibria for switching systems, which will be utilized in this paper [36].

Definition 3.1. A real (virtual) equilibrium $Z^* = (S^*_G, I^*_G)$ for system (3.3) is defined as follows: if Z^* is an equilibrium for subsystem S_{G_1} and $F(Z^*) < 0$ ($F(Z^*) \geq 0$), or if Z^* is an equilibrium for subsystem S_{G_2} and $F(Z^*) \geq 0$ ($F(Z^*) < 0$). Denoted the real (virtual) equilibrium Z^* by $E^r_{G_i}$ ($E^v_{G_i}$) for subsystem S_{G_i}, respectively. The real and virtual equilibria are all named regular equilibria.

3.1. Qualitative analysis of subsystem S_{G_1}

Given the biological significance of system (3.3), it is crucial to establish the existence of positive invariant sets for subsystem S_{G_1} to ensure the non-negativity of the system's solution.

Lemma 3.1. *The bounded set*

$$\Omega_1 = \left\{ (S_n^{G_1}, I_n^{G_1}) \middle| S_n^{G_1} > \max\{0, \frac{\mu + \delta + \gamma - 1}{\beta}\}, \ \ \Lambda > (\mu - 1 + \beta I_n^{G_1}) S_n^{G_1} \right\}$$

is a positive invariant set of subsystem S_{G_1}.

Proof. As $n = 0$, it follows from (3.1) and (3.4) that

$$\begin{cases} S_1^{G_1} = \Lambda + (1 - \beta I_0^{G_1} - \mu) S_0^{G_1}, \\ I_1^{G_1} = I_0^{G_1} [1 + \beta S_0^{G_1} - (\mu + \delta + \gamma)], \end{cases} \tag{3.6}$$

and $S_0^{G_1} > 0, I_0^{G_1} > 0$. In order to prove $S_1^{G_1} > 0$, it has got to prove

$$\Lambda > (\mu - 1 + \beta I_0^{G_1}) S_0^{G_1},$$

and this is our hypothesis.

To prove $I_1^{G_1} > 0$, it is obtained from the second formula of (3.6) that

$$1 + \beta S_0^{G_1} - (\mu + \delta + \gamma) > 0,$$

i.e.,

$$S_0^{G_1} > \frac{\mu+\delta+\gamma-1}{\beta}.$$

It is important to establish the relationship between 0 and $\frac{\mu+\delta+\gamma-1}{\beta}$, so we obtain that

$$S_0^{G_1} > \max\{0, \frac{\mu+\delta+\gamma-1}{\beta}\}.$$

Analogically, when $n = k$, if the conditions $S_k^{G_1} > \max\{0, \frac{\mu+\delta+\gamma-1}{\beta}\}$, $\Lambda > (\mu - 1 + \beta I_k^{G_1})S_k^{G_1}$ hold true, then we have $S_{k+1}^{G_1} > 0, I_{k+1}^{G_1} > 0$.

Hence, Ω_1 is the positive invariant set of S_{G_1}. The proof is completed.

The equilibrium of system S_{G_1} is determined by the following equations

$$\begin{cases} \Lambda - \beta S_n I_n - \mu S_n = 0, \\ \beta S_n I_n - (\mu+\delta+\gamma) I_n = 0. \end{cases} \tag{3.7}$$

Therefore, there is a disease-free equilibrium $P_1 = (\Lambda/\mu, 0)$. Let us define the basic reproduction number as $\mathcal{R}_0^{G_1} = \beta\Lambda/[\mu(\mu+\delta+\gamma)]$. Consequently, we can obtain the unique positive equilibrium

$$E_{G_1}^* = (S_{G_1}^*, I_{G_1}^*) = \left(\frac{\mu+\delta+\gamma}{\beta}, \frac{\Lambda}{\mu+\delta+\gamma} - \frac{\mu}{\beta}\right) = \left(\frac{\Lambda}{\mu\mathcal{R}_0^{G_1}}, \frac{\mu(\mathcal{R}_0^{G_1}-1)}{\beta}\right).$$

This completes the proof.

Next, we will explore the local stability of the positive equilibrium$(S_{G_1}^*, I_{G_1}^*)$.

Theorem 3.2. The positive equilibrium $E_{G_1}^* = (S_{G_1}^*, I_{G_1}^*)$ of system S_{G_1} is asymptotically stable, provided that

$$\max\left\{1, \frac{\mu(\mu+\delta+\gamma)-4}{\mu(\mu+\delta+\gamma)-2\mu}\right\} < \mathcal{R}_0^{G_1} < \frac{\mu+\delta+\gamma}{-1+\mu+\delta+\gamma}, \tag{3.8}$$

where

$$(\mu+\delta+\gamma) > \max\left\{2, \frac{4}{\mu}\right\}.$$

Proof.

The Jacobian Matrix J_1 of the equilibrium $E_{G_1}^* = (S_{G_1}^*, I_{G_1}^*)$ is

$$J_1 = \begin{bmatrix} 1-\mu-\beta I_{G_1}^* & -\beta S_{G_1}^* \\ \beta I_{G_1}^* & \beta S_{G_1}^* + 1 - (\mu+\delta+\gamma) \end{bmatrix}.$$

From Eq (3.7), we can acquire the characteristic equation for the Jacobian matrix J_1 of system S_{G_1} at $(S_{G_1}^*, I_{G_1}^*)$, and the characteristic equation is

$$P(\lambda) = \lambda^2 - (trJ_1)\lambda + detJ_1 \tag{3.9}$$

and

$$P(1) = 1 - trJ_1 + detJ_1 = \mu(\mathcal{R}_0^{G_1} - 1)(\mu+\delta+\gamma),$$

$$P(-1) = 1 + trJ_1 + detJ_1 = 4 - 2\mu\mathcal{R}_0^{G_1} + \mu(\mathcal{R}_0^{G_1} - 1)(\mu + \delta + \gamma).$$

Condition (3.8) ensures that inequalities

$$detJ_1 < 1, \quad P(1) > 0, \quad P(-1) > 0$$

hold. Using the Jury et al. [37], we can demonstrate that the modulus of all the roots of Eq (3.9) is less than 1, and the endemic equilibrium $E^*_{G_1} = (S^*_{G_1}, I^*_{G_1})$ is locally asymptotically stable.

3.2. Qualitative analysis of subsystem S_{G_2}

Similar to subsystem S_{G_1}, and considering the biological significance of the model, its solution must not be negative. Therefore, we have first derived the following results.

Lemma 3.3. *The bounded set*

$$\Omega_2 = \left\{(S_n^{G_2}, I_n^{G_2})\middle| e^{-mI_n^{G_2}} S_n^{G_2} > \max\{0, \frac{\mu + \delta + \gamma - 1}{\beta}\},\ \Lambda > (\mu - 1 + \beta e^{-mI_n^{G_2}} I_n^{G_2}) S_n^{G_2}\right\}$$

is a positive invariant set of subsystem S_{G_2}.

Since the proof method is similar to Lemma 3.1, we have omitted the proof process.

The equilibrium of system S_{G_2} is determined by the following equations

$$\begin{cases} \Lambda - \beta e^{-mI_n} S_n I_n - \mu S_n = 0, \\ \beta e^{-mI_n} S_n I_n - (\mu + \delta + \gamma) I_n = 0. \end{cases} \tag{3.10}$$

Obviously, system S_{G_2} exists a disease free equilibrium $P_2 = (\Lambda/\mu, 0)$, and the endemic equilibrium $E^*_{G_2} = (S^*_{G_2}, I^*_{G_2})$ satisfies

$$\Lambda - (\mu + \delta + \gamma) I^*_{G_2} - \frac{\mu(\mu + \delta + \gamma) e^{-mI^*_{G_2}}}{\beta} = 0.$$

Defining $x = I^*_{G_2}$, then

$$f(x) = ae^{mx} + bx + c = 0, \tag{3.11}$$

where

$$a = \frac{\mu(\mu + \delta + \gamma)}{\beta} > 0, \quad b = (\mu + \delta + \gamma) > 0, \quad c = -\Lambda < 0.$$

In addition, we study the positive equilibrium $(S^*_{G_2}, I^*_{G_2})$ of S_{G_2} by numerical methods. It follows from Eq (3.10) that

$$\Lambda - (\mu + \delta + \gamma) I^*_{G_2} = \frac{\mu(\mu + \delta + \gamma) e^{mI^*_{G_2}}}{\beta}. \tag{3.12}$$

Defining two auxiliary functions

$$\begin{cases} F(x) = \Lambda - (\mu + \delta + \gamma)x \\ G(x) = \dfrac{\mu(\mu + \delta + \gamma) e^{mI^*_{G_2}}}{\beta} \end{cases} \tag{3.13}$$

to verify the existence of an equilibrium for system S_{G_2}, Figure 1 shows $F(x)$ and $G(x)$ under different β. As $F(0) > G(0)$, two functions always intersect at a point, indicating the existence of the equilibrium

for subsystem S_{G_2}. The existence of an equilibrium in system S_{G_2} has been established, and its stability is now being investigated.

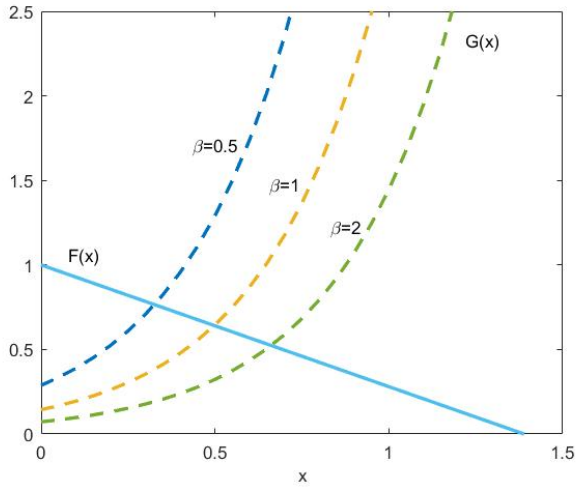

Figure 1. The existence of the equilibrium $(S^*_{G_2}, I^*_{G_2})$ of the subsystem $S^*_{G_2}$, parameters are $\Lambda = 1, \gamma = 0.5, \delta = 0.02, \mu = 0.2, m = 3$.

Theorem 3.4. *The positive equilibrium of system S_{G_2}, denoted by $E^*_{G_2} = (S^*_{G_2}, I^*_{G_2})$, is asymptotically stable provided that*

$$\begin{cases} \Lambda\beta e^{-mI^*_{G_2}} > \mu(\mu+\delta+\gamma)(1-mI^*_{G_2}), \\ (1-\dfrac{2}{\mu+\delta+\gamma})\Lambda\beta e^{-mI^*_{G_2}} > -4+\mu(\mu+\delta+\gamma)+(2-\mu)(\mu+\delta+\gamma)mI^*_{G_2}, \\ (1-\dfrac{1}{\mu+\delta+\gamma})\Lambda\beta e^{-mI^*_{G_2}} < \mu(\mu+\delta+\gamma)+(1-\mu)(\mu+\delta+\gamma)mI^*_{G_2}. \end{cases} \tag{3.14}$$

Proof. For the positive equilibrium $(S^*_{G_2}, I^*_{G_2})$ of the system S_{G_2}, we can get the characteristic equation of the Jacobian matrix J_2 for the subsystem S_{G_2} evaluated at $(S^*_{G_2}, I^*_{G_2})$.

$$P(\lambda) = \lambda^2 - (trJ_2)\lambda + detJ_2 \tag{3.15}$$

and

$$J_2 = \begin{bmatrix} 1-\mu-\beta e^{-mI^*_{G_2}} I^*_{G_2} & -\beta S^*_{G_2} e^{-mI^*_{G_2}}(1-mI^*_{G_2}) \\ \beta e^{-mI^*_{G_2}} I^*_{G_2} & \beta S^*_{G_2} e^{-mI^*_{G_2}}(1-mI^*_{G_2}) + 1 - (\mu+\delta+\gamma) \end{bmatrix}.$$

Clearly,

$$trJ_2 = 2 - \frac{1}{\mu+\delta+\gamma}\Lambda\beta e^{-mI^*_{G_2}} - (\mu+\delta+\gamma))mI^*_{G_2},$$

$$detJ_2 = 1 + (\mu-1)(\mu+\delta+\gamma)mI^*_{G_2} + (1-\frac{1}{\mu+\delta+\gamma})\Lambda\beta e^{-mI^*_{G_2}} - \mu(\mu+\delta+\gamma).$$

According to the Jury et al. [37], the condition for the local stability of the equilibrium $E^*_{G_2}$ is

$$|trJ_2| < detJ_2 + 1 < 2. \tag{3.16}$$

Conditions (3.14) guarantee the validity of the inequality (3.16), which implies that the endemic disease equilibrium $(S^*_{G_2}, I^*_{G_2})$ of subsystem S_{G_2} is locally asymptotically stable.

4. Dynamical behavior of the Filippov system

In this section, we will study the complex dynamics of the infectious disease switching system (3.3). This is a complex, nonlinear dynamic system with a threshold strategy, making it difficult to analyze in detail theoretically. Therefore, we will analyze the bifurcation [38–40] of parameters and the outbreak state under the influence of initial density by numerical simulations.

4.1. Equilibria bifurcation for the switching system (3.3)

Based on Definition 3.1, this section mainly focuses on the real and virtual equilibrium states of the two subsystems in system (3.3) and conducts a dynamic behavior analysis on them through numerical simulations. To clearly demonstrate the existence of various equilibrium parameter spaces, we have selected γ and ET as bifurcation parameters while fixing other parameters, as shown in Figure 2. Observing the parameter space plane when ET ranges from 0 to 6 and γ ranges from 0 to 1, it is divided into five regions. When the recovery rate γ is within the range of $[0, 0.325] \cup [0.725, 1]$, two regions can be identified: region I-1 only has the existence of $E^r_{G_1}$, while region I-2 only has the existence of $E^v_{G_1}$. In the case of intermediate recovery rates ($\gamma \in [0.325, 0.725]$), it can be observed that $E^r_{G_1}$ and $E^r_{G_2}$ coexist in II-1, $E^v_{G_1}$ and $E^r_{G_2}$ coexist in II-2, and $E^v_{G_1}$ and $E^v_{G_2}$ coexist in II-3. Figure 2 displays various bifurcaiton phenomena, which provide important insights into how to hold back the disease outbreaks or control the density of infected individuals in areas below the threshold ET. Through numerical analysis, we can select an appropriate threshold ET such that the equilibrium state of subsystem S_{G_2} is a virtual equilibrium state, which can help us achieve our control objectives.

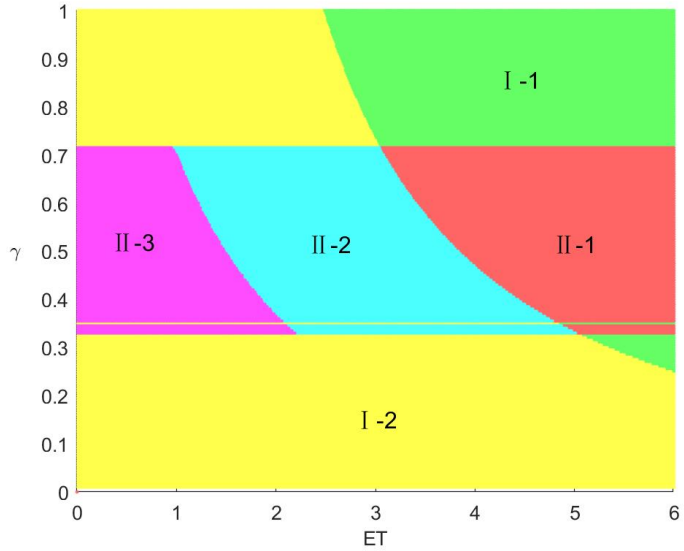

Figure 2. Bifurcation diagram for the existence of equilibria of model (3.3) to γ and ET, other parameters are $\Lambda = 1.8, m = 0.4, \beta = 0.06, \mu = 0.05, \delta = 0.05$.

4.2. Bifurcation analysis about sensitive parameters

Codimension-1 bifurcation analysis is a common method to obtain a preliminary understanding of dynamic behavior. It provides information about the influence of a specific parameter on dynamics. We

analyze the codimension one bifurcation diagrams of the parameters μ, δ, and β separately to observe the type of attractor and its change with the variation of the parameter.

First, we select μ as the bifurcation parameter to study the complex dynamic behavior of system (3.3) while fixing other parameters as shown in Figure 3. When μ increases from 0.863 to 0.902, periodic solutions, chaotic solutions, and periodic doubling solutions can be observed. Further, as the parameter μ changes from 0.8656 to 0.8783, the solution of system (3.3) becomes stable. Notably, at $\mu = (0.8827, 0.8958)$, the system exhibits an obvious chaotic state. The bifurcation diagram illustrates that small perturbations in parameters can lead to significant changes in the system's dynamic behavior.

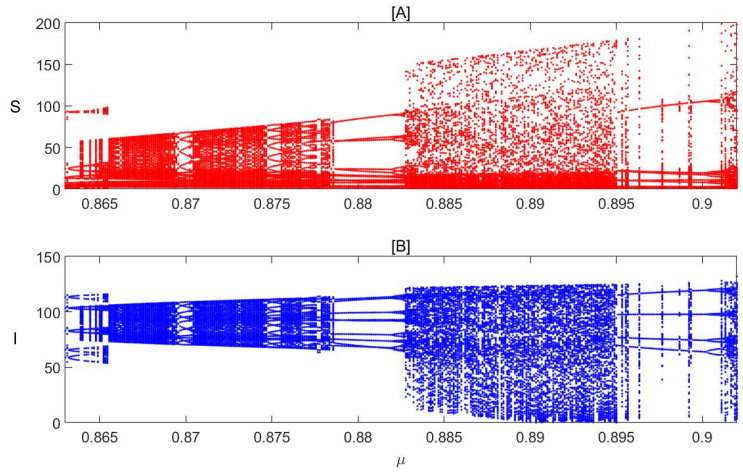

Figure 3. Bifurcation diagram for model (3.3) concerning μ. All other parameters are as follows: $\Lambda = 0.9, ET = 1, m = 0.04, \beta = 0.0009, \delta = 1.187, \gamma = 0.1$.

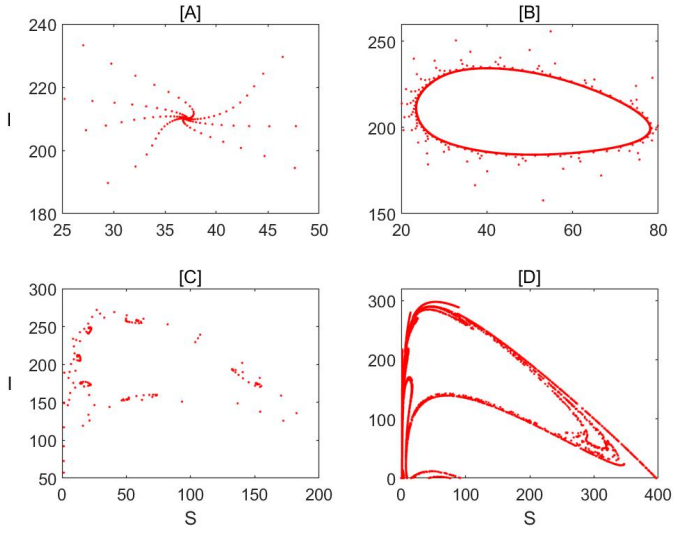

Figure 4. Phase-plan of model (3.3) with different δ. All other parameters are as follows: $\Lambda = 0.9, ET = 1, m = 0.01, \beta = 0.004, \mu = 0.81, \gamma = 0.1$, and [A] $\delta = 1.18$, [B] $\delta = 1.2$, [C] $\delta = 1.22$, [D] $\delta = 1.252$.

Second, building upon the bifurcation Figure 3, we held other parameters constant and explored various states of the system's solutions by selecting different values of δ, as shown in Figure 4. When $\delta = 1.18$ in Figure 4 (A), system (3.3) has a stable solution. However, when δ increases from 1.18 to 1.2, the system exhibits a periodic solution, as shown in Figure 4(B). As δ reaches 1.22 or 1.252, a chaotic solution abruptly emerges, as depicted in Figure 4 (C),(D). As the parameter continues to change, the nature of the system's solutions undergoes fundamental shifts, highlighting the significant influence of parameters on the system.

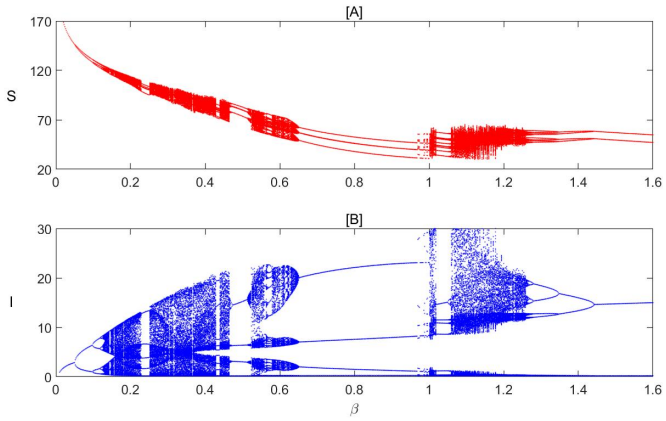

Figure 5. Bifurcation diagram for model (3.3) concerning β. All other parameters are as follows: $\Lambda = 10, \mu = 0.049, ET = 3, \gamma = 0.9, \delta = 0.04, m = 0.7$.

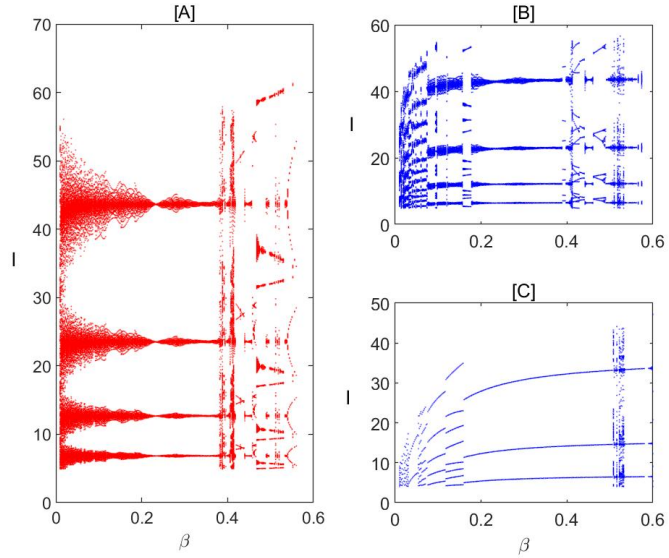

Figure 6. Bifurcation diagram for model (3.3) concerning β. All other parameters are as follows: $\Lambda = 10, ET = 9, m = 0.7, \delta = 0.03, \gamma = 0.43$, and [A] $\mu = 0.001$, [B] $\mu = 0.01$, [C] $\mu = 0.1$.

Third, we investigate β in the system as the bifurcation parameter, while keeping other parameters unchanged. Figure 5 exhibitions that the system exhibits very complex dynamic behaviors when β increases. In particular, in the interval of $\beta \in (0, 1.6)$, the system displays period-doubling branches,

chaotic solutions and periodic solutions. In Figure 5, the system (3.3) exhibits multiple periodic and chaotic solutions, such as for $\beta \in [0.04, 0.652] \cup [0.99, 1.45]$. This highlights the available impact of the infection rate on disease transmission.

To further understand the influence of parameter μ on the system in this state, we explore values between 0.01 and 0.6, as shown in Figure 6, and observe that different natural mortality rates can affect the system's dynamic behavior. The bifurcation diagrams of system (3.3) with respect to β under the influence of μ become increasingly simpler, as depicted in Figures 6 (A)–(C).

4.3. Initial sensitivities

In addition to the significant and sensitive parameters that have a crucial impact on disease transmission, the initial density of susceptible and infected individuals in a given area can also have varying effects on the outbreak state of the disease. This section systematically investigates the dynamic behavior of the switching system (3.3) under different initial conditions.

To investigate the interaction between initial density and media factors, we fix the parameter values as shown in Figure 7 and analyze the different scenarios presented by different initial densities. In Figure 7(A), with an initial density of (13,1.7), the numerical simulation results show that the density of infected individuals never exceeds the given $ET = 2$, indicating that media factors are not required to control the outbreak.

However, for initial densities of (12,1.5) or (11.7,2), the results indicate that the system will be affected by media factors once or twice, and the density of infected individuals will stabilize in the system area, as shown in Figure 7(B), (C). On the other hand, when the initial density is (11,1), society must strengthen public's attention and protective measures through the influence of media factors multiple times to keep the density of infected individuals below ET.

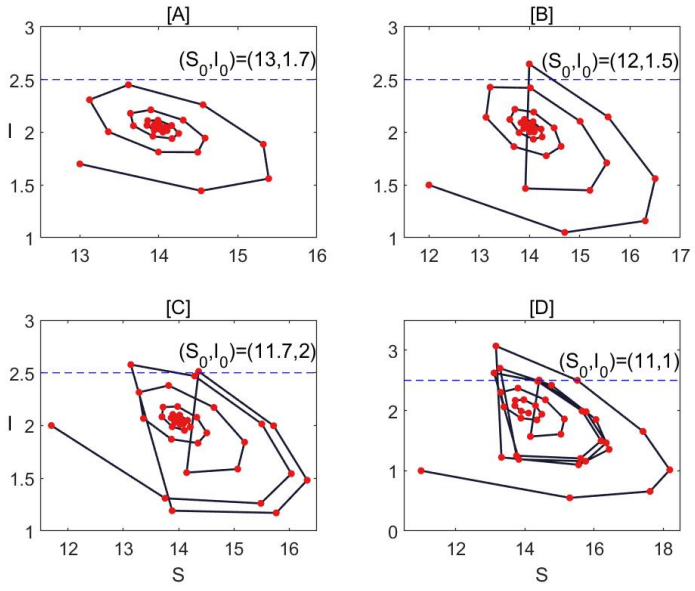

Figure 7. Switching impact of model (3.3) under different initial densities. All other parameters are as follows: $\Lambda = 12, ET = 2.5, m = 0.09, \mu = 0.55, \delta = 1.25, \gamma = 0.3$, and [A] $(S_0, I_0) = (13, 1.7)$, [B] $(S_0, I_0) = (12, 1.5)$, [C] $(S_0, I_0) = (11.7, 2)$, [D] $(S_0, I_0) = (11, 1)$.

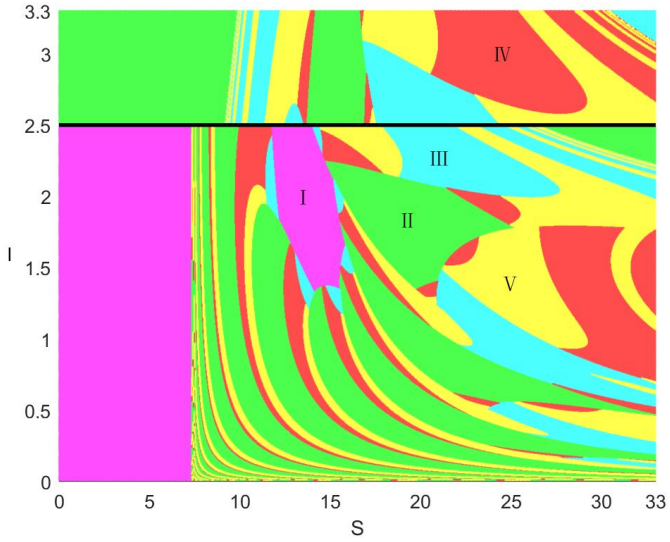

Figure 8. The frequency of disease outbreaks at the initial density (S_0, I_0) of the system (3.3). All other parameters are as follows: $\Lambda = 12, ET = 2.5, \mu = 0.55, \delta = 1.25, \gamma = 0.3, m = 0.09, \beta = 0.15$.

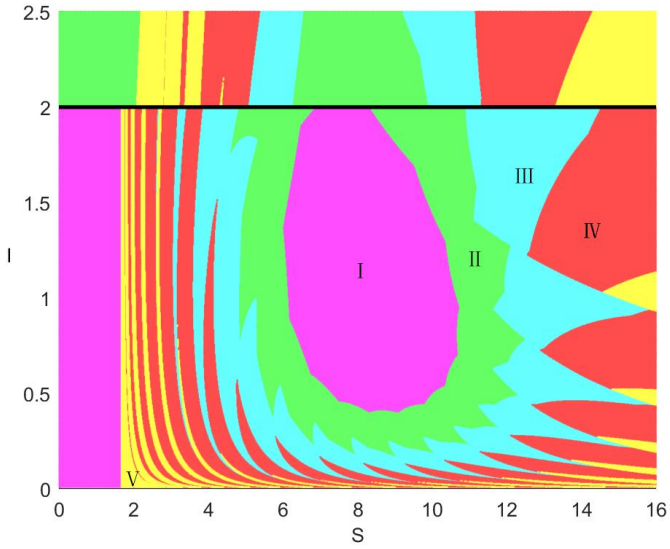

Figure 9. The frequency of disease outbreaks at the initial density (S_0, I_0) of the system (3.3). All other parameters are as follows: $\Lambda = 1.7, ET = 2, \mu = 0.05, \delta = 1.2, \gamma = 0.3, m = 0.11, \beta = 0.15$.

Furthermore, we analyzed the effect of the initial population density on the outbreak of infectious diseases by creating a horizontal classification map of susceptibles and infected individuals while keeping other parameters fixed (see Figure 7). As shown in Figure 8, infectious diseases will not break out in region I, and the impact of media reports on the population is minimal since the disease is not serious. In green zone II, an outbreak will occur when the initial population density is within a certain range. As the number of infected people exceeds the threshold, media coverage will play

a role in preventing susceptible groups from being infected and controlling the spread of infectious diseases. There will be two outbreaks in area III, and the media needs to repeatedly emphasize and remind everyone to pay attention to it. Eventually, there will be no further outbreaks. The solution of the system in area IV will not be affected by media factors after three outbreaks, while the solution in area V will experience more than three outbreaks. Clearly, when the number of infected people exceeds ET, different initial population densities within a certain range will lead to varying outbreak frequencies of infectious diseases. Similarly, when we vary the values of other parameters, we can also observe similar phenomena, as shown in Figure 9.

Based on the above analysis, it can be inferred that the initial population density plays a crucial role in disease outbreaks, and monitoring population density in endemic areas can be beneficial for preventing and controlling infectious diseases.

4.4. Multiple attractors and coexistence

As previously mentioned, the switching system for infectious diseases reveals various dynamic behaviors, including the coexistence of multiple attractors. To better understand its biological significance, we selected different initial densities while fixing other parameters, as shown in Figure 10.

For instance, when $m = 0.066$, two infectious disease outbreak attractors exist simultaneously, exhibiting different outbreak frequencies and amplitudes (i.e., Figure 10(A),(B). On one hand, if the initial values (S_0, I_0) are set to $(7.9, 1.91)$, the attractor exhibits the amplitude and frequency shown in Figure 10(A), which is approximated by the solution of system (3.3). On the other hand, when the initial values (S_0, I_0) change to $(9, 1.8)$, the amplitudes and frequencies become different from those in Figure 10(A), displaying a more complex burst pattern, as shown in Figure 10(B).

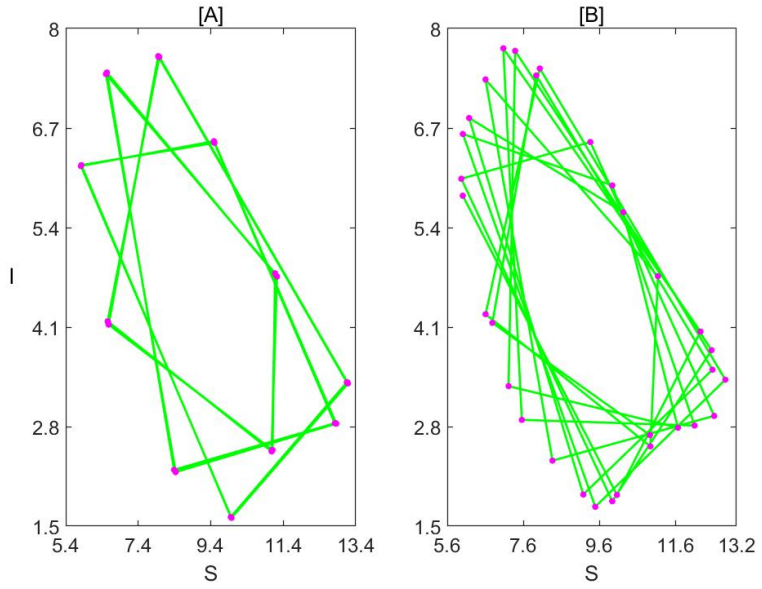

Figure 10. Coexisting attractors of model (3.3) with different initial values. All other parameters are as follows: $\Lambda = 16, ET = 2, \beta = 0.3, \mu = 0.8, \delta = 1, \gamma = 0.1$; [A] $(S_0, I_0) = (7.9, 1.91)$, [B] $(S_0, I_0) = (9, 1.8)$.

Figure 11 illustrates three periodic outbreak attractors with different amplitudes and periods, which are selected by fixing three population inputs. If we fix the initial population density as $(100, 10)$, the three attractors coexist and exhibit different amplitudes and frequencies with different values of population inputs. Corresponding to $\Lambda = 130, 150, 300$, we can observe that the three attractors have different periods of 3, 6 and 5, respectively. In particular, the periodic attractor in the third condition has the largest amplitude for both susceptible and infected persons, and the outbreak pattern is the most complex. In the first case, the outbreak pattern is similar to that in the second case, but the outbreak cycle is very different.

Based on the analysis of attractors in Figures 10 and 11, it is evident that the initial densities and population inputs of susceptible and infected individuals may lead to different intervention strategies for controlling the outbreak of an epidemic. Therefore, in addition to monitoring population density in endemic areas, it is also necessary to consider population movements.

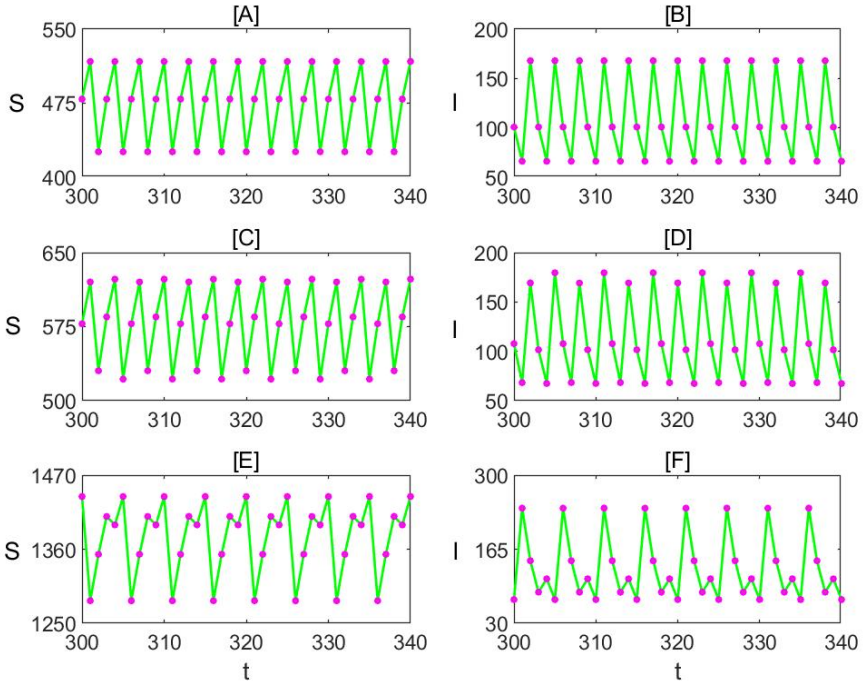

Figure 11. Coexisting attractors of model (3.3) with different Λ. All other parameters are as follows: $(S_0, I_0) = (100, 10), ET = 15, m = 0.1, \beta = 2.8, \mu = 0.18, \gamma = 0.12, \delta = 0.1$; [A,B] $\Lambda = 130$, [C,D] $\Lambda = 150$, [E,F] $\Lambda = 300$.

Furthermore, the initial density also impacts the switching frequency of the infectious disease switching system (3.3), as depicted in Figure 12 (A)–(C). Notably, Figure 12 (A)–(C) underwent 13 and 15 switching events, respectively. Figure 12 (D)–(F) illustrate the correlation between switching time and frequency corresponding to Figure 12 (A)–(C), respectively.

The switching frequency in Figure 12 (D) initially stabilized at 5, subsequently fluctuating within the range of [4,9], but with an overall increasing trend. The switching frequency in Figure 12 (E) remained at 5 during the fourth switching and decreased to 4 during the final switching. The switching frequency in Figure 12 (F) also stabilized at 5 and then rose to 9 during the last switching event. Elevated system

switching occurrences imply a need for more frequent implementation of control measures. This, in turn, indirectly escalates media coverage frequency and the associated reporting costs. Consequently, accounting for the initial value becomes imperative when devising strategies for managing infectious diseases.

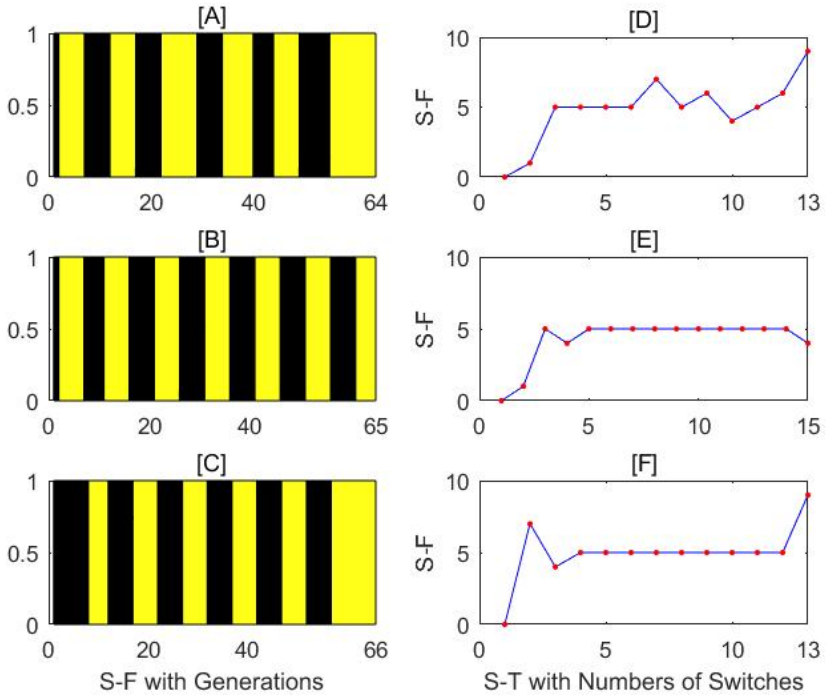

Figure 12. Switching frequency (S–F) and switching time (S–T) of system (3.3). Parameters are $ET = 10, m = 0.1, \beta = 0.3, \mu = 0.8, \gamma = 0.1, \delta = 1, \Lambda = 15$. The initial densities from top to bottom are (3.88, 7.95), (4.61, 5.47) and (7.25, 4.71).

5. Concluding remarks

In this paper, we research the dynamics model of infectious disease affected by media reports and the threshold of infected persons. We derived and established a discrete switching infectious disease model and performed a qualitative analysis of its subsystem. The dynamic behavior of the model was analyzed using various methods, including codimension two bifurcation diagrams, codimension one bifurcation diagrams and initial sensitivity. We found that multiple parameters and population density in an area can influence infectious disease outbreaks under the influence of vectors, providing important information for the eradication of infectious diseases. Our results highlight the need to consider media reports and population movements when monitoring and controlling infectious diseases. To explore the dynamic behavior of the model, we employ qualitative analysis techniques related to differential equations to study the existence and stability of equilibria in the subsystems. Using codimension two bifurcation analysis, we identify regions where the system has true and false equilibria, as shown in Figure 2. Based on these findings, a reasonable threshold ET can be designed for preventing and treating infectious diseases to maintain a stable true equilibrium in system (3.1) and a virtual equilibrium in system (3.2), thereby promoting disease eradication.

Since various parameters can potentially affect the dynamic behavior of the system, we analyzed the possible bifurcation behavior of system (3.3) as shown in Figures 3–6, which exhibits a variety of dynamic behaviors such as periodic and chaotic solutions, multistability and period doubling bifurcations. The branching diagram reveals that the path to chaos is very intricate, demonstrating that hidden factors such as infection rate, natural mortality, mortality due to disease, etc., affect the dynamic behavior of the system. The media reports influence factor m indirectly affects the changes in these factors. This illustrates that people's influence through media reports can increase awareness of prevention and lead to corresponding preventive and control measures, thereby reducing the spread of diseases. Furthermore, we also explored the relationship between the initial population density and the prevention of infectious diseases. Figures 7–9 provide evidence that changes in population density, under the influence of media reports, can cause different disease outbreaks through the codimension two bifurcation map and the codimension one bifurcation map. Furthermore, Figure 10 shows that different population densities, when the fixed m remains unchanged, will produce different attractors and the complexity of system dynamics will also differ. The coexistence of three attractors in Figure 11 also reflects that different population inputs lead to similar phenomena. Therefore, reasonable and effective monitoring and control of population densities and inputs in epidemic areas, under the influence of the media, is conducive to prevent and control the infectious diseases.

Moreover, we have presented the switching frequency and switching time of the system (3.3) under various initial conditions, highlighting the relationship between initial density and the control of infectious diseases. The results demonstrate that the initial density of susceptible and infected individuals influences the ultimate state following the onset of infectious diseases, as illustrated in Figure 12. The variability in switching frequencies further reinforces this observation. Hence, incorporating the initial value becomes a significant aspect in the study of infectious disease switching systems.

We have investigated the dynamic behavior of the infectious disease switching system under the influence of media coverage. However, the limitation of medical resources also affects the speed and efficiency of disease control. If the maximum hospital capacity is significantly lower than the threshold of media response, it would be crucial to incorporate the resource limitation into the infectious disease switching model. This is an important topic for future research both theoretically and practically. Furthermore, for comparative analysis, regarding the continuous counterpart of the discrete switching infectious disease model, we will employ the Filippov switching model to depict it. We will provide corresponding comparative studies as well. This is a meaningful topic that deserves further in-depth investigation.

Use of AI tools declaration

The author declares that no AI tools were utilized for data analysis, modeling, or decision-making processes.

Acknowledgements

This work is supported by National Natural Science Foundation of China (No. 12261104, 12361104), and the Youth Talent Program of Xingdian Talent Support Plan (XDYC-QNRC-2022-0708).

References

1. Q. Gan, R. Xu, Y. Li, R. Hu, Travelling waves in an infectious disease model with a fixed latent period and a spatio–temporal delay, *Math. Comput. Model.*, **53** (2011), 814–823. https://doi.org/10.1016/j.mcm.2010.10.018
2. M. Y. Li, Z. Shuai, C. Wang, Global stability of multi-group epidemic models with distributed delays, *J. Math. Anal. Appl.*, **361** (2010), 38–47. https://doi.org/10.1016/j.jmaa.2009.09.017
3. A. B. Gumel, S. Ruan, T. Day, J. Watmough, F. Brauer, P. Van den, et al., Modelling strategies for controlling SARS outbreaks, *Proc. R. Soc. Lond. B.*, **271** (2004), 2223–2232. https://doi.org/10.1098/rspb.2004.2800
4. M. Premkumar, D. Devurgowda, S. Dudha, R. Maiwall, C. Bihari, S. Grover, et al., A/H1N1/09 influenza is associated with high mortality in liver cirrhosis, *J. Clin. Exp. Hepato.*, **9** (2019), 162–170. https://doi.org/10.1016/j.jceh.2018.04.006
5. J. Deng, S. Tang, H. Shu, Joint impacts of media, vaccination and treatment on an epidemic filippov model with application to covid-19, *J. Theor. Biol.*, **523** (2021), 110698. https://doi.org/10.1016/j.jtbi.2021.110698
6. C. Q. Ling, Complementary and alternative medicine during covid-19 pandemic: What we have done, *J. Integr. Med.*, **20** (2022), 1–3. https://doi.org/10.1016/j.joim.2021.11.008
7. S. T. M. Thabet, M. S. Abdo, K. Shah, T. Abdeljawad, Study of transmission dynamics of covid-19 mathematical model under abc fractional order derivative, *Results Phys.*, **19** (2020), 103507. https://doi.org/10.1016/j.rinp.2020.103507
8. S. Bhattacharya, S. Paul, The behaviour of infection, survival and testing effort variables of SARS-CoV-2: A theoretical modelling based on optimization technique, *Results Phys.*, **19** (2020), 103568. https://doi.org/10.1016/j.rinp.2020.103568
9. Z. E. Ma, Y. C. Zhou, W. D. Wang, Z. Jin, *Mathematical modeling and, research on the dynamics of infectious diseases*, Science Press, Beijing, 2004.
10. A. Misra, A. Sharma, J. Shukla, Modeling and analysis of effects of awareness programs by media on the spread of infectious diseases, *Math. Comput. Model.*, **53** (2011), 1221–1228. https://doi.org/10.1016/j.mcm.2010.12.005
11. G. P. Sahu, J. Dhar, Dynamics of an SEQIHRS epidemic model with media coverage, quarantine and isolation in a community with pre-existing immunity, *J. Math. Anal. Appl.*, **421** (2015), 1651–1672. https://doi.org/10.1016/j.jmaa.2014.08.019
12. V. Capasso, G. Serio, A generalization of the kermack-mckendrick deterministic epidemic model, *Math. Biosci.*, **42** (1978), 43–61. https://doi.org/10.1016/0025-5564(78)90006-8
13. J. A. Cui, X. Tao, H. Zhu, An sis infection model incorporating media coverage, *Rocky Mountain J. Math.*, **38** (2008), 1323–1334.
14. J. M. Tchuenche, N. Dube, C. P. Bhunu, R. J. Smith, C. T. Bauch, The impact of media coverage on the transmission dynamics of human influenza, *BMC Public Health*, **11** (2011), 1–14. https://doi.org/10.1186/1471-2458-11-S1-S5

15. J. M. Tchuenche, C. T. Bauch, Dynamics of an infectious disease where media coverage influences transmission, *Int. Scholarly Res. Notices*, **2012** (2012). https://doi.org/10.5402/2012/581274

16. Z. Sun, H. Zhang, Y. Yang, H. Wan, Y. Wang, Impacts of geographic factors and population density on the covid-19 spreading under the lockdown policies of China, *Sci. Total Environ.*, **746** (2020), 141347. https://doi.org/10.1016/j.scitotenv.2020.141347

17. A. Misra, S. N. Mishra, A. L. Pathak, P. K. Srivastava, P. Chandra, A mathematical model for the control of carrier-dependent infectious diseases with direct transmission and time delay, *Chaos Soliton. Fract.*, **57** (2013), 41–53. https://doi.org/10.1016/j.chaos.2013.08.002

18. T. Tonia, Social media in public health: is it used and is it useful?, *Int. J. Public Health*, **59** (2014), 889–891. https://doi.org/10.1007/s00038-014-0615-1

19. R. Liu, J. Wu, H. Zhu, Media/psychological impact on multiple outbreaks of emerging infectious diseases, *Comput. Math. Methods Med.*, **8** (2007), 153–164.

20. J. Cui, Y. Sun, H. Zhu, The impact of media on the control of infectious diseases, *J. Dyn. Diff. Equations*, **20** (2008), 31–53. https://doi.org/10.1007/s10884-007-9075-0

21. J. Liu, X. Liu, W. C. Xie, Input-to-state stability of impulsive and switching hybrid systems with time-delay, *Automatica*, **47** (2011), 899–908. https://doi.org/10.1016/j.automatica.2011.01.061

22. P. Mason, U. Boscain, Y. Chitour, Common polynomial lyapunov functions for linear switched systems, *SIAM J. Control and Optim.*, **45** (2006), 226–245. https://doi.org/10.1137/040613147

23. Y. Xiao, T. Zhao, S. Tang, Dynamics of an infectious diseases with media/psychology induced non-smooth incidence, *Math. Biosci. Eng.*, **10** (2013), 445–461. http://dx.doi.org/10.3934/mbe.2013.10.445

24. Y. Liu, Y. Xiao, An epidemic model with saturated media/psychological impact, *Appl. Math. Mech.*, **34** (2013), 399–407.

25. M. Zhao, *Qualitative and quantitative study of a non-smooth filippov epidemical model with threshold strategy*, Master thesis, Xi'an University of Science and Technology in Xi'an, 2018.

26. Z. Hu, Z. Teng, L. Zhang, Stability and bifurcation analysis in a discrete SIR epidemic model, *Math. Comput. Simul.*, **97** (2014), 80–93. https://doi.org/10.1016/j.matcom.2013.08.008

27. Y. Enatsu, Y. Nakata, Y. Muroya, G. Izzo, A. Vecchio, Global dynamics of difference equations for SIR epidemic models with a class of nonlinear incidence rates, *J. Diff. Equations Appl.*, **18** (2012), 1163–1181.

28. V. I. Utkin, Sliding modes and their applications in variable structure systems, *Mir Moscow*, (1978).

29. V. I. Utkin, Scope of the theory of sliding modes, in *Sliding Modes in Control and Optimization*, Springer, (1992), 1–11. https://doi.org/10.1007/978-3-642-84379-2_1

30. W. O. Kermack, A. G. McKendrick, A contribution to the mathematical theory of epidemics, *Proc. R. Soc. Lond. A.*, **115** (1927), 700–721. https://doi.org/10.1098/rspa.1927.0118

31. L. J. Allen, Some discrete-time SI, SIR, and SIS epidemic models, *Math. Biosci.*, **124** (1994), 83–105. https://doi.org/10.1016/0025-5564(94)90025-6

32. C. Castillo-Chavez, A. A. Yakubu, Dispersal, disease and life-history evolution, *Math. Biosci.*, **173** (2001), 35–53. https://doi.org/10.1016/S0025-5564(01)00065-7

33. Y. Zhou, P. Fergola, Dynamics of a discrete age-structured SIS models, *Discrete Cont. Dyn. Syst. B*, **4** (2004), 841–850. https://doi.org/10.3934/dcdsb.2004.4.841

34. X. Hu, W. Qin, M. Tosato, Complexity dynamics and simulations in a discrete switching ecosystem induced by an intermittent threshold control strategy, *Math. Biosci. Eng.*, **17** (2020), 2164–2179.

35. Y. Xiao, S. Tang, J. Wu, Media impact switching surface during an infectious disease outbreak, *Sci. Rep.*, **5** (2015), 1–9. https://doi.org/10.1038/srep07838

36. C. Xiang, Z. Xiang, S. Tang, J. Wu, Discrete switching host-parasitoid models with integrated pest control, *Int. J. Bifurcat. Chaos*, **24** (2014), 1450114. https://doi.org/10.1142/S0218127414501144

37. E. Jury, L. Stark, V. Krishnan, Inners and stability of dynamic systems, *IEEE Trans. Syst. Man Cybern.*, **10** (1976), 724–725.

38. Y. Lv, L. Chen, F. Chen, Z. Li, Stability and bifurcation in an SI epidemic model with additive allee effect and time delay, *Int. J. Bifurcat. Chaos*, **31** (2021), 2150060. https://doi.org/10.1142/S0218127421500607

39. W. Yin, Z. Li, F. Chen, M. He, Modeling allee effect in the leslie-gower predator–prey system incorporating a prey refuge, *Int. J. Bifurcat. Chaos*, **32** (2022), 2250086. https://doi.org/10.1142/S0218127422500869

40. T. Liu, L. Chen, F. Chen, Z. Li, Dynamics of a leslie–gower model with weak allee effect on prey and fear effect on predator, *Int. J. Bifurcat. Chaos*, **33** (2023), 2350008. https://doi.org/10.1142/S0218127423500086

AIMS Press